Bifidobacterium adolescentis improves lifespan and healthspan by regulating catalase activity and oxidative stress-associated metabolites

Shujie Chen
Department of Gastroenterology, Sir Run Run Shaw Hospital, Zhejiang University School of Medicine
Luyi Chen
Department of Gastroenterology, Sir Run Run Shaw Hospital, Zhejiang University School of Medicine
Yadong Qi
Department of Gastroenterology, Sir Run Run Shaw Hospital, Zhejiang University School of Medicine
Jilei Xu
Department of Gastroenterology, Sir Run Run Shaw Hospital, Zhejiang University School of Medicine
Qiwei Ge
Department of Gastroenterology, Second Affiliated Hospital, Zhejiang University School of Medicine
Yuedan Fan
Department of Neurobiology and Department of Neurosurgery of the First Affiliated Hospital, Zhejiang University School of Medicine
Du Chen
Department of Neurobiology and Department of Neurosurgery of the First Affiliated Hospital, Zhejiang University School of Medicine
Yawen Zhang
Department of Gastroenterology, Sir Run Run Shaw Hospital, Zhejiang University School of Medicine
Lan Wang
Department of Gastroenterology, Sir Run Run Shaw Hospital, Zhejiang University School of Medicine
Tongyao Hou
Department of Gastroenterology, Sir Run Run Shaw Hospital, Zhejiang University School of Medicine
Xiaohang Yang
Institute of Genetics and Department of Genetics, Division of Human Reproduction and Developmental Genetics of the Women's Hospital, Zhejiang University
Yongmei Xi
Institute of Genetics and Department of Genetics, Division of Human Reproduction and Developmental Genetics of the Women's Hospital, Zhejiang University
Jianmin Si
Department of Gastroenterology, Sir Run Run Shaw Hospital, Zhejiang University School of Medicine
Lijun Kang

Department of Neurobiology and Department of Neurosurgery of the First Affiliated Hospital, Zhejiang University School of Medicine

Liangjing Wang (wangljzju@zju.edu.cn)

Second Affiliated Hospital, Zhejiang University School of Medicine

Article

Keywords: Fecal Microbiota Sequencing, Osteoporosis, Neurodegeneration, Cellular Senescence, Host Metabolism

Posted Date: October 20th, 2020

DOI: https://doi.org/10.21203/rs.3.rs-90247/v1

Abstract

Microbiota-host interaction was involved in aging, while the specific bacterium was undetermined. To identify candidate bacterium with aging, we performed fecal microbiota sequencing. Less richness of gut microbial community, and a reduction of *B.adolescentis* abundance was observed in elderly individuals. *B. adolescentis* supplement improved osteoporosis and neurodegeneration in telomerase RNA component deletion ($Terc^{-/-}$) aged mice. *B.adolescentis* induced prolongevity and healthspan improvement in *Drosophila melanogaster* and *C. elegans*. Transgenic deletion of *ctl-2* in *C. elegans* abolished the effect on lifespan and healthspan by *B. adolescentis*. The catalase activity was decreased in skeletal muscle and brain tissues of $Terc^{-/-}$ mice, as well as cellular senescence in mouse embryonic fibroblasts. *B. adolescentis* alleviated ROS accumulation by regulation of oxidative stress-associated metabolites. These results suggest a role for *B. adolescentis* in improving lifespan and healthspan by regulating catalase activity and host metabolism. Supplement with commensal bacteria is a promising strategy against age related diseases.

Main Manuscript

Aging is a process and status of holistic host organs, characterized as physiological function deterioration, cellular function decline underpins the development of pathological alterations[1]. Studies have been conducted to extend lifespan or induce healthy aging in different model organisms, ranging from yeast, zebra fish, worms, flies to mice[2–4]. As the largest component of host microbiota, gut microbes have been proved to function in a variety of physiological and pathological processes. Recent studies demonstrated that fecal microbiota transplantation could extend lifespan and healthspan in progeria mice[5]. Studies have been performed on the elderly or centenarian populations through 16S rRNA, metagenomic or metatranscriptomic shotgun sequencing to distinguish the compositional and functional alteration of gut microbiota with aging[6–8]. However, biological effect of specific commensal bacteria on aging and the potential mechanisms were unclear.

Here, we observed that the abundance of *Bifidobacterium adolescentis* (*B. adolescentis*) exhibited a significant decline in elderly populations by fecal microbiota sequencing, which was confirmed in 3500 samples from GMrepo database. *B. adolescentis* supplement improved age-related osteoporosis and neurodegeneration in telomerase RNA component deletion ($Terc^{-/-}$) aged mice, as well as inducing lifespan prolongation and healthspan improvement in nonmammalian organisms *Drosophila melanogaster* and *Caenorhabditis elegans*. The anti-aging effect of *B. adolescentis* was regulated by the activity of catalase and oxidative stress-associated metabolites.

Results

Gut microbiota diversity and B. adolescentis **abundance decreased with aging**

To investigate the change of gut microbiota with aging, we performed 16S rRNA sequencing of fecal samples. 166 participants were divided into three groups according to chronological age (Supplementary Table 1**)**. We found that alpha-diversity estimators shannon index and heip index of human gut microbiota significantly decreased from the younger to the elderly populations (Fig. 1A,B), indicating less richness of gut microbiota with aging. A remarkable reduction of *Firmicutes*, *Actinobacteria*, *Saccharibacteria*, together with an increment of *Fusobacteria*, were detected with age at phylum level (Fig. 1C). The composition of gut microbiota didn't change with age in a linear association[6]. In addition, an increment of *Bacteroidetes*:*Firmicutes* (B:F) ratio and a shift of butyrate-producing bacteria were observed in centenarians[6,7]. We observed that 45 KEGG pathways indispensable for maintaining lifespan, including 28 metabolism-associated pathways were differentially enriched with aging. Most metabolism-associated pathways were predicted to be more active in elderly individuals, such as lipopolysaccharide biosynthesis, N-glycan biosynthesis, glutathione metabolism and amino acid metabolism (Supplementary Fig. 1). Collectively, gut microbiota profiles altered with aging and might participate in the regulation of host metabolism.

We subsequently performed linear discriminant analysis (LDA) coupled with effect size measurements to screen out candidate bacteria (Fig. 1D). Notably, the *B. adolescentis* distribution was the most significant difference between two groups (Supplementary Table 2). Short chain fatty acids (SCFAs) were recognized as beneficial bacterial metabolites which were important for host metabolism. We found that relative abundance of bacterial taxa associated with SCFA production, such as *B. adolescentis, Ruminococcaceae*, *Faecalibacterium prausnitzi* and *Eubacterium ractale*, was significantly decreased in elderly individuals while *B. adolescentis* exhibited most prominent reduction (Fig. 1E). Furthermore,relative abundance of *B. adolescentis* was confirmed to be significant higher in younger individuals by qPCR assay (Fig. 1F). Similar result was obtained by analyzing GMrepo sequencing database between young and old ages (n = 2821 vs. n = 679 samples) (Fig. 1G). As reported in previous study, microbiota in aged people has displayed reduction in the abundance of several bacteria with anti-inflammatory and immunomodulatory properties, including *Bifidobacterium, Akkermansia, Lactobacillus* and *Christensenellaceae*[9]. Taken together, we concluded that the abundance of *B. adolescentis* was decreased with aging and *B. adolescentis* might play pivotal role in the regulation of healthy aging .

Oral gavage with B. adolescentis **alleviated aged related osteoporosis and neurodegeneration in Terc$^{-/-}$ progeroid mice**

Telomerase, consisting of three main components, is essential for maintaining telomere length and plays an important role in tissue renewal and organism lifespan[10]. Telomerase RNA component deletion (Terc$^{-/-}$) mice with C57BL/6 background show progressive telomere shortening from first generation (G1) until the third (G3) generation, which exhibits significant phenotype of premature aging[11–13]. To verify the effect of *B. adolescentis* on age, Terc$^{-/-}$ G3 progeroid mice of 6–8 weeks age were oral gavaged with *B. adolescentis* for five months, while wild-type Terc$^{+/+}$ mice were gavaged with PBS as control (Fig. 2A). The body weight of Terc$^{-/-}$ mice was significantly lower than those of wild-type Terc$^{+/+}$ mice, whereas *B.*

adolescentis supplement significantly increased body weight as compared to control group (Fig. 2B). Frailty index score, which comprehensively quantified frailty in aged mice[14], exhibited remarkable difference between wild-type and Terc$^{-/-}$ mice gavaged with PBS. *B. adolescentis* supplement improved age related frailty index in Terc$^{-/-}$ mice (Fig. 2C).

Aging has been characterized by multiple organic dysfunction, including musculoskeletal and neurodegenerative diseases[15,16]. To assess the biological effect of *B. adolescentis* on bone density, we performed micro-CT scan and three-dimensional reconstruction of femora in mice. The bone volume/total volume (BV/TV) and trabecular thickness (Tb.Th) of Terc$^{-/-}$ mice were significantly decreased as compared to wild-type mice. These indices in Terc$^{-/-}$ mice were increased after gavaged with *B. adolescentis* (Fig. 2D), which suggested *B. adolescentis* supplement could improve osteoporosis in aged Terc$^{-/-}$ mice. Previous study showed that neurodegenerative changes in brain was linked with gut microbiota[17]. We then assessed senescence status by comparing the morphological changes and surviving number of neurons in the CA3 region of hippocampus in mice (Fig. 2E). Nuclear deviation, cytoplasm condensed and nuclear fragmented of neurons were more prominent in Terc$^{-/-}$ mice than those of control group, and the surviving number of neurons in mice gavaged with *B. adolescentis* also showed a significant increase compared to controls. Collectively, these results indicated that supplement with *B. adolescentis* improved healthspan in Terc$^{-/-}$ progeroid mice.

B. adolescentis **supplement improved lifespan and healthspan in** D. melanogaster **and** C. elegans

Invertebrate organisms such as the fruit fly *D. melanogaster* and the nematode *C. elegans* with a relative short lifespan, availability of different genetic mutants and morphological and functional similarities of gut were broadly used as proof-of-concept models on microbiome-aging studies[18–20]. Some bacterial strains, such as *Comamonas* DA1877 and *Lactobacillus gasseri* SBT2055, have been identified to influence the lifespan and reproduction of *C. elegans* by regulating series of signaling pathways[21–23]. We administrated *B. adolescentis* and conventional food to *D. melanogaster* and *C. elegans*, and comprehensively verify the effect of *B. adolescentis* on the lifespan and healthspan of the two organisms. Wild-type *D. melanogaster* strains (both w^{1118} and Canton-S) supplemented with *B. adolescentis* both showed a significant increase of lifespan (Fig. 3A,B), approximately 20% increment was observed (Supplementary Table 3). Then we tested healthspan parameters of flies on day 30. The climbing ability of female w^{1118} supplemented with *B. adolescentis* was improved as compared to control group (Fig. 3C). Canton-S flies supplemented with *B. adolescentis* exhibited stronger creep ability than controls as well (Fig. 3D).

The lifespan of *C. elegans* was also significantly improved when supplied with *B. adolescentis* with different mixture ratios (Fig. 4A). 1:1 mixture with *B. adolescentis* and *E. coli* OP50 can significantly improve the mean maximum lifespan of *C. elegans* (Fig. 4B). In addition, the locomotion ability of aged worms was significantly enhanced (Fig. 4C,D). We observed that the heat stress resistance was obviously changed with *B. adolescentis* supplement (Fig. 4E). Healthspan was further evaluated by

autofluorescence quantification of intestinal lipofuscin, which accumulated with age (Fig. 4F) The autofluorescence intensity of worms in *B. adolescentis* intervention group was significantly lower than that of control group (Fig. 4G). Collectively, *B. adolescentis* supplement could improve lifespan and healthspan in both *D. melanogaster* and *C. elegans*.

ctl-2 is essential for B. adolescentis-induced lifespan extension and healthspan improvement in C. elegans

To elucidate the mechanisms of *B. adolescentis*-induced lifespan improvement, genes expression involved in lifespan were evaluated in *C. elegans* and *D. melanogaster*. Expression of *sod-3* and *ctl-2* was significantly higher in *C. elegans* supplemented with *B. adolescentis* than control group (Fig. 5A). Similar result was observed in flies considering corresponding homologous gene *sod-3* and *cat* (Supplementary Fig. 2A,B). To clarify the gene involved in lifespan, experiments of corresponding mutants were performed in *C. elegans.* Interestingly, *B. adolescentis* supplement could still extend the lifespan in *C. elegans* carried with *sod-3* mutant, while the lifespan prolongation was abolished in *ctl-2* mutant (Fig. 5B-D). To validate this finding, we constructed transgenic worms and detected the expression of *ctl-2* directly with mCherry fluorescence. The *ctl-2* expression was significantly increased with *B. adolescentis* supplement in aged worms (Fig. 5E,F). We then detected healthspan indicators aforementioned in *ctl-2* mutant *C. elegans*. The enhancement of locomotion ability by *B. adolescentis* was blocked in *ctl-2* mutant (Fig. 5G). Similarly, no significant improvement of survival time was observed in *ctl-2* mutant with *B. adolescentis* supplement (Fig. 5H). Moreover, the autofluorescence intensity was increased in *ctl-2* mutants group (Fig. 5I,J). In conclusion, *B. adolescentis* supplement could prolong lifespan and improve healthspan of *C. elegans* through the regulation of *ctl-2*.

B. adolescentis suppressed aged Terc$^{-/-}$ G3 mice by regulating the activity of catalase and oxidative stress-associated metabolites

The activity of catalase (CAT), which was homologous to *C. elegans ctl-2* gene, was subsequently detected in muscle and brain tissue of mice. Terc$^{-/-}$ aged mice exhibited decreased activity of CAT compared to wild-type mice, and *B. adolescentis* supplement significantly enhanced the activity of CAT (Fig. 6A). In addition, *B. adolescentis*-gavaged Terc$^{-/-}$ aged mice showed prominent increased protein expression of CAT in muscle and brain tissues (Fig. 6B,C and Supplementary Fig. 3A). Immunohistochemistry staining revealed that *B. adolescentis* supplement exhibited downregulation of p53, while upregulation of CAT, in cortex and hippocampus regions (Fig. 6D and Supplementary Fig. 3B). These results demonstrated that *B. adolescentis* supplement suppressed aged related phenotype in Terc$^{-/-}$ G3 mice by regulating CAT.

To verify the effect of *B. adolescentis in vitro*, *B. adolescentis* was then administrated to culture medium in both replicative and DOX-induced senescent MEFs. *B. adolescentis* supplement significantly suppressed cellular senescence as shown by senescence-associated β-galactosidase staining (Fig. 6E,F

and Supplementary Fig. 4A,B). In line with observation in mice, the mRNA and protein expression level of CAT was upregulated by *B. adolescentis* in senescent MEFs (Fig. 6G,H and Supplementary Fig. 4C).

Finally, we performed metabolomics analysis of mice feces to evaluate the effect of *B. adolescentis* on oxidative stress-associated metabolites as CAT was an important ROS scavenger[24]. In accordance with our findings in brain and muscle tissues, apiin and erucic acid, which could increase the activity of CAT[25–27], were significantly enriched in the feces of *B. adolescentis*-gavaged Terc$^{-/-}$ aged mice. Some other antioxidants also exhibited enrichment with *B. adolescentis* supplement, including ginsenoside Ia[28], 2-hydroxycinnamic acid[29], daidzin[30] and L-malic acid[31], while ROS producer such as hypoxanthine[32] was reduced. Furthermore, several metabolites with proinflammatory property or associated with cardiovascular diseases were enriched in Terc$^{-/-}$ aged mice, including cholic acid[33], 9,10-DHOME[34], 3-dehydroxycarnitine[35] and 4-trimethylammoniobutanoic acid[36]. Cosmosiin[37] with anti-aging potential and enterodiol[38] with tumor-suppression activity were enriched in *B. adolescentis*-gavaged Terc$^{-/-}$ aged mice (Fig. 7A-C). Collectively, these results indicated that *B. adolescentis* supplement suppressed aged Terc$^{-/-}$ mice and MEFs cellular senescence by regulating CAT and oxidative stress-associated metabolites.

Discussion

Gut microbial community was changed with aging, and the abundance of *B. adolescentis* elicited a dramatic decline in elderly, which was supported by sequencing results in 3500 fecal samples from GMrepo database. Several bacteria have been previously identified to be related with aging and played critical role in aging prediction, such as family *Ruminococcaceae*, genera *Alistipes*, *Bacteroides*, *Bifidobacterium*, *Faecalibacterium*, *Akkermansia*, *Roseburia* and *Eubacterium*[9,39,40]. Transplantation with the gut microbiota of old donor mice to young germ-free mice exhibited age-sensitive enrichment in butyrate-producing microbes[41]. We observed that oral gavaged with *B. adolescentis* induced lifespan extension and healthspan improvement in both Terc$^{-/-}$ mice, and nonmammalian model organisms such as worms and flies. Transplantation with the *Akkermansia muciniphila* was sufficient to exert beneficial healthspan effects in two progeroid mouse models of Hutchinson–Gilford progeria syndrome[5]. These results demonstrate the association between aging and the gut microbiota, and provide experimental evidence with commensal bacteria against age-related diseases.

Gut microbiota communicates with host organs through bacterial structural product, nutrient-metabolites and complex pathways. Development of series organic dysfunction was demonstrated to be associated with gut microbiota, including neurodegenerative diseases[16,42], osteoporosis[43,44], diabetes mellitus[45], nonalcoholic fatty liver disease[46,47] and cardiovascular disease[48]. Microbiota dysbiosis has been linked with disruption of intestinal barrier integrity and gut inflammation. Wang *et al.* demonstrated that *Lactobacillus paracasei* D3-5 and lipoteichoic acid from its cell wall could ameliorate aging-related leaky gut and inflammation by modulating TLR-2/MAPK/NF-kB pathway[49]. High-throughput lifespan-associated screening on *C. elegans* uncovered that 29 *E. coli* mutants and bacterial metabolite polysaccharide colonic acid were involved in the prolongevity process[50]. Transplant of *Akkermansia*

muciniphila had beneficial effects in progeroid mice by reestablishing healthy microbiome through restoring secondary bile acids[5]. In present study, we observed that the accumulation of intestine lipofuscin, a lipid peroxidation product, was significantly reduced in *B. adolescentis*-treated *C. elegans*. Furthermore, *B. adolescentis* supplement in Terc$^{-/-}$ mice regulated lipid metabolism and oxidative stress-associated metabolites. In the prediction of human gut microbiota function, endocytosis and phagocytosis were predicted to be more active in younger populations. Hence, we can hypothesize that probiotics may regulate age-related disorders through gut inflammation and host metabolism.

To gain an insight into the underlying mechanisms, we identified candidate *ctl-2* gene function in Terc$^{-/-}$ mice, *C. elegans* and senescent MEFs supplemented with *B. adolescentis*. Studies have shown that *ctl-2* accounts for the majority of catalase activity in nematodes, and lack of *ctl-2* can lead to the premature aging of nematodes[51]. As an important substance in living organisms, catalase is participating in the process of active oxygen metabolism. Under environmental stress, ROS resulted in cell membrane damage, DNA damage and subsequent cell senescence[24]. Pathogenic microbes have been reported to impair intestinal cell repair and shorten host lifespan by generation of ROS in flies[52]. A recent study demonstrated that preventing ROS accumulation in gut allows survival without sleep in flies[53]. We found that the catalase activity in muscle and brain was upregulated by supplementation with *B. adolescentis* in Terc$^{-/-}$ mice, which was supported by the metabolomic analysis of mice feces. Metabolites facilitating the activity of CAT together with other antioxidants were enriched in *B. adolescentis*-gavaged Terc$^{-/-}$ mice, which could remarkably reduce the intracellular ROS level. In addition, erucic acid, cosmosiin and 2-hydroxycinnamic acid have been proposed as potential therapeutic agents for Alzheimer disease by ameliorating nueroinflammation and blocking neural cell death[27,29,37]. Daidzin could inhibit LPS-induced bone loss by suppressing the osteoclast differentiation[54]. The enrichment of these metabolites may underlie the improvement of phenotype in Terc$^{-/-}$ mice supplemented with *B. adolescentis*.

In conclusion, we showed that *B. adolescentis* exerted beneficial effects on lifespan and healthspan by the regulating of catalase activity and host metabolism. The underlying molecular mechanisms should be further explored.

Methods

Study design

The objectives of this study was to screen out candidate beneficial bacterium and elucidate its functional characteristics on aging and prolongevity. Fecal samples were collected from healthy volunteers and 16S rRNA sequencing was performed. Microbiota data obtained from GMrepo metagenomes database were used to confirm the *B. adolescentis* abundance in different age. Next, age-related phenotype was conducted in Terc$^{-/-}$ aged mice, *D. melanogaster* and *C. elegans* with *B. adolescentis* supplement. Micro-CT bone scan and staining in hippocampal CA3 region was evaluated in Terc$^{-/-}$ aged mice gavaged with *B. adolescentis*. Lifespan was recorded and series healthspan indices

were measured, which including mean survival time, frailty index score, locomotion ability and intestinal lipofuscin accumulation. For further mechanism exploration, lifespan assay on *C. elegans* carried with serial gene mutants were performed with *B. adolescentis* supplement. Lastly, expression of *ctl-2* homologous gene catalase (CAT) was detected in muscle and brain tissues from $Terc^{-/-}$ aged mice, as well as in senescent MEFs cells by qRT-PCR, western blot and immunohistochemistry assays. Metabolomics of mice feces were performed to analyze effect of *B. adolescentis* on gut microbial metabolites. Researchers were blinded to group allocation, and mice, flies and worms were randomized to groups. All procedures were conducted in compliance with institutional guidelines and were approved by the Animal Ethical Committee of Zhejiang University prior to initiating the study.

Healthy subjects and fecal samples collection

Healthy subjects aged over 18 years old were recruited at Sir Run Run Shaw Hospital (Zhejiang Province, China) from December 2016 to December 2018. Admission criteria were listed as follows: without history of digestive tract-related diseases such as intestinal adenoma and tumors; without thyroid disease or diabetes mellitus; no use of antibiotics or probiotics in the past month; BMI between 18.5 and 24.9 kg/m^2; women are not in pregnant or lactation period. Fresh stool samples were collected, immediately frozen and stored at -80°C before DNA isolation. This study was approved by the Ethics Committee of Sir Run Run Shaw Hospital, College of Medicine, Zhejiang University (20161206-21). Written informed consent was obtained from all participants before enrollment.

16S rRNA sequencing

Microbial DNA from stool samples was isolated with TIANamp Stool DNA Kit (TIANGEN BIOTECH, Beijing, China) according to the manufacturer's instructions. The V3-V4 hypervariable regions of 16S rRNA gene were amplified and purified amplicons were paired-end sequenced on an Illumina MiSeq platform according to the standard protocols by Majorbio Bio-Pharm Technology Co. Ltd. (Shanghai, China). Bacterial taxonomy determination and functional predictions were performed as earlier described[55].

Online database resources

Microbiota online data were obtained from GMrepo, an metagenomes database of human gut[56]. Using python software through RESTful APIs, we obtained relative abundance of *B. adolescentis* in samples with healthy phenotype of in all age groups from GMrepo. 3500 samples were included for final analysis.

$Terc^{+/-}$ mice and aged related phenotype

$Terc^{+/-}$ G0 mice (C57BL/6 background), gift from Prof. Zhangfa Song (Zhejiang University), were intercrossed to generate $Terc^{+/+}$ (wild-type C57BL/6) and $Terc^{-/-}$ G1 mice. Genotype identification was conducted by agarose gel electrophoresis (Supplementary Fig. 5). Then $Terc^{-/-}$ G1 mice were intercrossed to generate $Terc^{-/-}$ G3 mice. 6-8-week-old wild-type C57BL/6 littermates were gavaged with PBS (WT+PBS, n=11). 6-8-week-old $Terc^{-/-}$ G3 littermates were randomly assigned to PBS group (G3+PBS, n=9) and *B. adolescentis* group (G3+*B.a*, n=12). Body weight and frailty index score were recorded monthly according to previous study [14] until natural death or sacrifice at 7 months old. All mice were housed at Sir Run Run Shaw Hospital animal facility in a pathogen-free level room. The room temperature was maintained at 20-22°C with 12-h light/dark cycle. Mice were provided with food and water ad libitum.

Micro-CT imaging

The left bones of mice were isolated and the attachments of the left femora muscle were removed. Three femora samples of each group were randomly selected and scanned by micro-CT (InspeXio SMX-225 CT FPD HR; Shimadzu Co. Ltd., Kyoto, Japan) after fixation in 4% paraformaldehyde overnight. Each sample was reconstructed using micro-CT software (VGStudio MAX; Volume Graphics, Heidelberg, Germany) under the same conditions. A region of intersect (ROI) cube was taken underneath epiphyseal growth plate. The reconstruction parameters of bone volume/total volume (BV/TV) and trabecular thickness (Tb.Th) were analyzed.

Lifespan assay

For lifespan assay, flies were allowed to develop and mate for 4~6 days after eclosion. Then they were starved for 2h in an empty vial, sexually segregated and randomly assigned to intervention or control vials. Every 20 flies were flipped to a vial and transferred to new vials every 2 or 3 days. The number of dead flies were counted simultaneously. About 100 flies (5 vials) were used each assay.

For *C. elegans*, L4 stage (day 0) worms were cultured in OP50 plates until maturation and then transferred to OP50 or mixture plates.150 worms were distributed in 10 plates (15 worms/plate), and incubated at 20 °C. The worms were transferred to new freshly seeded plates every other day. The number of alive or dead worms were counted on every transfer day.

Survival rates were calculated as the percentage of surviving flies/worms versus the total number of flies/worms. Flies that lost and worms died as a result of getting stuck to the wall of the plate were excluded from the analysis. The evaluation of lifespan was performed at least three times.

C. eleganselegans fluorescence microscopy

Worms were synchronized and cultured as described in online supplementary materials and methods. On day 10 and 14, the lipofuscin accumulation in worm intestine and *ctl-2* expression were quantified with autofluorescence and mCherry red fluorescence, respectively. Worms were randomly selected and wash twice with M9 buffer. Then they were mounted on a slide coated with 200mM sodium azide to induce anesthesia and photos were taken under blue excitation light (405~488 nm) or red excitation light (559-585 nm) with inverted laser scanning confocal microscope (Olympus IX81-FV1000, Tokyo, Japan). Fluorescence was quantified with ImageJ (National Institutes of Health, Bethesda, MD, USA). Three independent experiments were conducted with >20 worms.

C. elegans gene integration

Promoter *ctl-2* and *ctl-2* gDNA were PCR-amplified from N2 genomic DNA and then recombined with specific donor vector fragments using In-Fusion PCR Cloning Kit (TaKaRa, Japan). To measure the expression level of *ctl-2* gene, a functional *Pctl-2::ctl-2 gDNA::mCherry* transgene was made by cloning the mCherry reporter sequence in frame and downstream of the *ctl-2* gDNA sequence. Transgenic animals were generated by micro-injecting *Pctl-2::ctl-2 gDNA::mCherry* transgene (50 ng/μL) mixed with a co-injection marker *Plin-44::gfp* (20 ng/μL). Gene integration was performed by ultraviolet trimethylpsoralen (UV-TMP) treatment and the integrated worms were backcrossed four times with N2.

Metabolomics analysis

Metabolites from mice fecal samples were extracted according to the standard protocols by Biotree Biological Technology Co. Ltd. (Shanghai, China). LC-MS/MS analyses were performed using an UHPLC system (Vanquish, Thermo Fisher Scientific) with a UPLC BEH Amide column (2.1 mm × 100 mm, 1.7 μm) coupled to Q Exactive HFX mass spectrometer (Orbitrap MS, Thermo). The raw data were converted to the mzXML format using ProteoWizard and processed with an in-house program, which was developed using R and based on XCMS, for peak detection, extraction, alignment, and integration. Then an in-house MS2 database (BiotreeDB) was applied in metabolite annotation. The cutoff for annotation was set at 0.3. Details were described in online supplementary materials and methods.

Statistical analysis

Differences of three groups were analyzed by one-way analysis of variance (ANOVA) for data with normal distribution or Kruskal-Wallis test for data with non-normal distribution. Differences of two groups were analyzed by Student's t-test or nonparametric tests (Wilcoxon rank sum test or Kruskal-Wallis test). For lifespan assays, log-rank (Mantel-Cox) test was performed. All statistical tests were two-tailed, and p-values <0.05 were considered statistically significant. Analysis and figures were performed using IBM SPSS Statistics V22.0 software, GraphPad Prism v7 and Image J (https://imagej.nih.gov/ij/; RRID:SCR_003070).

Data availability

All data supporting the findings of the present study are available within this article and the Supplementary Information files. Raw 16S rRNA sequencing data files are available in the Sequence Read Archive (SRA) database under the accession number PRJNA625181 (http://www.ncbi.nlm.nih.gov/bioproject/625181).

Declarations

Competing interests statement

The authors declare no competing interests.

Author Contributions

SC, LW, LK, JS, XY and YX conceived the research idea and designed the study; SC, LC, YQ and JX carried out experiments; LC, LW and YZ collected clinical samples; SC, LC, YQ, JX, QG, YF, DC, TH performed data analysis; SC and LC wrote the manuscript with input from coauthors. All authors critically revised and approved the final version of the manuscript.

Acknowledgements

We thank Prof. Xin Wang and Prof. Wei Liu (Zhejiang Academy of Agricultural Sciences, China) for sharing the anaerobic operating system and guiding on bacteria culture; Prof. Zhangfa Song (Zhejiang University, China) for kindly providing Terc$^{+/-}$ G0 mice; Prof. Fei Xu (Zhejiang University, China) for helpful discussion. This project was supported by the National Foundation of Natural Science of China (82072623, 31800878, 31900736) and National Key R&D Program of China (2016YFC1303200).

References

1. Bana, B. & Cabreiro, F. The Microbiome and Aging. *Annu Rev Genet* **53**, 239–261.
2. Carmona-Gutierrez, D. *et al.* The flavonoid 4,4'-dimethoxychalcone promotes autophagy-dependent longevity across species. *Nat Commun* **10**, 651.
3. Eisenberg, T. *et al.* Induction of autophagy by spermidine promotes longevity. *Nat Cell Biol* **11**, 1305–1314.
4. Obata, F., Fons, C. O. & Gould, A. P. Early-life exposure to low-dose oxidants can increase longevity via microbiome remodelling in Drosophila. *Nat Commun* **9**, 975.

5. Barcena, C. *et al.* Healthspan and lifespan extension by fecal microbiota transplantation into progeroid mice. *Nat Med* **25**, 1234–1242.
6. Biagi, E. *et al.* Through ageing, and beyond: gut microbiota and inflammatory status in seniors and centenarians. *PLoS One* **5**, e10667.
7. Wang, F. *et al.* Gut Microbiota Community and Its Assembly Associated with Age and Diet in Chinese Centenarians. *J Microbiol Biotechnol* **25**, 1195–1204.
8. Kim, B. S. *et al.* Comparison of the Gut Microbiota of Centenarians in Longevity Villages of South Korea with Those of Other Age Groups. *J Microbiol Biotechnol* **29**, 429–440.
9. Ruiz-Ruiz, S. *et al.* Functional microbiome deficits associated with ageing: Chronological age threshold. *Aging Cell* **19**, e13063.
10. Blasco, M. A. *et al.* Telomere shortening and tumor formation by mouse cells lacking telomerase RNA. *Cell* **91**, 25–34.
11. Roberts, A. R. *et al.* Non-telomeric epigenetic and genetic changes are associated with the inheritance of shorter telomeres in mice. *Chromosoma* **122**, 541–554.
12. Perez-Rivero, G. *et al.* Mice deficient in telomerase activity develop hypertension because of an excess of endothelin production. *Circulation* **114**, 309–317.
13. Bernardes de Jesus, B. *et al.* The telomerase activator TA-65 elongates short telomeres and increases health span of adult/old mice without increasing cancer incidence. *Aging Cell* **10**, 604–621.
14. Whitehead, J. C. *et al.* A clinical frailty index in aging mice: comparisons with frailty index data in humans. *J Gerontol A Biol Sci Med Sci* **69**, 621–632.
15. McHugh, D. & Gil, J. Senescence and aging: Causes, consequences, and therapeutic avenues. *J Cell Biol* **217**, 65–77.
16. Kritsilis, M. *et al.* Ageing, Cellular Senescence and Neurodegenerative Disease. *Int J Mol Sci* **19**.
17. Kundu, P., Blacher, E., Elinav, E. & Pettersson, S. Our Gut Microbiome: The Evolving Inner Self. *Cell* **171**, 1481–1493.
18. Zhang, R. & Hou, A. Host-Microbe Interactions in Caenorhabditis elegans. *ISRN Microbiol* 2013, 356451.
19. Kumar, A. *et al.* Caenorhabditis elegans: a model to understand host-microbe interactions. *Cell Mol Life Sci* **77**, 1229–1249.
20. Ren, C., Webster, P., Finkel, S. E. & Tower, J. Increased internal and external bacterial load during Drosophila aging without life-span trade-off. *Cell Metab* **6**, 144–152.
21. MacNeil, L. T., Watson, E., Arda, H. E., Zhu, L. J. & Walhout, A. J. Diet-induced developmental acceleration independent of TOR and insulin in C. elegans. *Cell* **153**, 240–252.
22. Garsin, D. A. *et al.* Long-lived C. elegans daf-2 mutants are resistant to bacterial pathogens. *Science* **300**, 1921.
23. Nakagawa, H. *et al.* Effects and mechanisms of prolongevity induced by Lactobacillus gasseri SBT2055 in Caenorhabditis elegans. *Aging Cell* **15**, 227–236.

24. Davalli, P., Mitic, T., Caporali, A., Lauriola, A. & D'Arca, D. ROS, Cell Senescence, and Novel Molecular Mechanisms in Aging and Age-Related Diseases. *Oxid Med Cell Longev* 2016, 3565127.
25. Li, P. *et al.* In vitro and in vivo antioxidant activities of a flavonoid isolated from celery (Apium graveolens L. var. dulce). *Food Funct* **5**, 50–56.
26. Altinoz, M. A. & Ozpinar, A. PPAR-delta and erucic acid in multiple sclerosis and Alzheimer's Disease. Likely benefits in terms of immunity and metabolism. *Int Immunopharmacol* **69**, 245–256.
27. Kim, E. *et al.* The memory-enhancing effect of erucic acid on scopolamine-induced cognitive impairment in mice. *Pharmacol Biochem Behav* **142**, 85–90.
28. Li, J. *et al.* Effective-component compatibility of Bufei Yishen formula II inhibits mucus hypersecretion of chronic obstructive pulmonary disease rats by regulating EGFR/PI3K/mTOR signaling. *J Ethnopharmacol* **257**, 112796.
29. Hao, S. *et al.* Hydroxycinnamic Acid from Corncob and Its Structural Analogues Inhibit Abeta40 Fibrillation and Attenuate Abeta40-Induced Cytotoxicity. *J Agric Food Chem* **68**, 8788–8796.
30. Wu, K. C., Chiang, B. J., Tsai, W. H., Chung, S. D. & Chien, C. T. I-Tiao-Gung extract through its active component daidzin improves cyclophosphamide-induced bladder dysfunction in rat model. *Neurourol Urodyn* **37**, 2560–2570.
31. Stoyanova, S., Geuns, J., Hideg, E. & Van den Ende, W. The food additives inulin and stevioside counteract oxidative stress. *Int J Food Sci Nutr* **62**, 207–214.
32. Quinlan, G. J., Lamb, N. J., Tilley, R., Evans, T. W. & Gutteridge, J. M. Plasma hypoxanthine levels in ARDS: implications for oxidative stress, morbidity, and mortality. *Am J Respir Crit Care Med* **155**, 479–484.
33. Yamada, S. *et al.* Cholic Acid Enhances Visceral Adiposity, Atherosclerosis and Nonalcoholic Fatty Liver Disease in Microminipigs. *J Atheroscler Thromb* **24**, 1150–1166.
34. Apaya, M. K. *et al.* Simvastatin and a Plant Galactolipid Protect Animals from Septic Shock by Regulating Oxylipin Mediator Dynamics through the MAPK-cPLA2 Signaling Pathway. *Mol Med* **21**, 988–1001.
35. Rombouts, C. *et al.* Untargeted metabolomics of colonic digests reveals kynurenine pathway metabolites, dityrosine and 3-dehydroxycarnitine as red versus white meat discriminating metabolites. *Sci Rep* **7**, 42514.
36. Drouin, N. *et al.* Electromembrane Extraction of Highly Polar Compounds: Analysis of Cardiovascular Biomarkers in Plasma. *Metabolites* **10**.
37. min, Z. *et al.* Cosmosiin Increases ADAM10 Expression via Mechanisms Involving 5'UTR and PI3K Signaling. *Front Mol Neurosci* **11**, 198.
38. Shin, M. K., Jeon, Y. D. & Jin, J. S. Apoptotic effect of enterodiol, the final metabolite of edible lignans, in colorectal cancer cells. *J Sci Food Agric* **99**, 2411–2419.
39. Biragyn, A. & Ferrucci, L. Gut dysbiosis: a potential link between increased cancer risk in ageing and inflammaging. *Lancet Oncol* **19**, e295-e304.

40. Moya, A. & Ferrer, M. Functional Redundancy-Induced Stability of Gut Microbiota Subjected to Disturbance. *Trends Microbiol* **24**, 402–413.
41. Kundu, P. *et al.* Neurogenesis and prolongevity signaling in young germ-free mice transplanted with the gut microbiota of old mice. *Sci Transl Med* **11**.
42. Sherwin, E., Bordenstein, S. R., Quinn, J. L., Dinan, T. G. & Cryan, J. F. Microbiota and the social brain. *Science* **366**.
43. Li, L. *et al.* Microbial osteoporosis: The interplay between the gut microbiota and bones via host metabolism and immunity. *Microbiologyopen* **8**, e00810.
44. Biver, E. *et al.* Gut microbiota and osteoarthritis management: An expert consensus of the European society for clinical and economic aspects of osteoporosis, osteoarthritis and musculoskeletal diseases (ESCEO). *Ageing Res Rev* **55**, 100946.
45. Forslund, K. *et al.* Disentangling type 2 diabetes and metformin treatment signatures in the human gut microbiota. *Nature* **528**, 262–266.
46. Caussy, C. & Loomba, R. Gut microbiome, microbial metabolites and the development of NAFLD. *Nat Rev Gastroenterol Hepatol* **15**, 719–720.
47. Henao-Mejia, J. *et al.* Inflammasome-mediated dysbiosis regulates progression of NAFLD and obesity. *Nature* **482**, 179–185.
48. Tang, W. H. W., Backhed, F., Landmesser, U. & Hazen, S. L. Intestinal Microbiota in Cardiovascular Health and Disease: JACC State-of-the-Art Review. *J Am Coll Cardiol* **73**, 2089–2105.
49. Wang, S. *et al.* Lipoteichoic acid from the cell wall of a heat killed Lactobacillus paracasei D3-5 ameliorates aging-related leaky gut, inflammation and improves physical and cognitive functions: from C. elegans to mice. *Geroscience*.
50. Han, B. *et al.* Microbial Genetic Composition Tunes Host Longevity. *Cell* **169**, 1249–1262 e1213.
51. Petriv, O. I. & Rachubinski, R. A. Lack of peroxisomal catalase causes a progeric phenotype in Caenorhabditis elegans. *J Biol Chem* **279**, 19996–20001.
52. Lee, K. A. *et al.* Bacterial-derived uracil as a modulator of mucosal immunity and gut-microbe homeostasis in Drosophila. *Cell* **153**, 797–811.
53. Vaccaro, A. *et al.* Sleep Loss Can Cause Death through Accumulation of Reactive Oxygen Species in the Gut. *Cell* **181**, 1307–1328 e1315.
54. Wei, G. *et al.* Daidzin inhibits RANKL-induced osteoclastogenesis in vitro and prevents LPS-induced bone loss in vivo. *J Cell Biochem* **120**, 5304–5314.
55. Chen, L. *et al.* The impact of Helicobacter pylori infection, eradication therapy and probiotic supplementation on gut microenvironment homeostasis: An open-label, randomized clinical trial. *EBioMedicine* **35**, 87–96.
56. Wu, S. *et al.* GMrepo: a database of curated and consistently annotated human gut metagenomes. *Nucleic Acids Res* **48**, D545-D553.

Figures

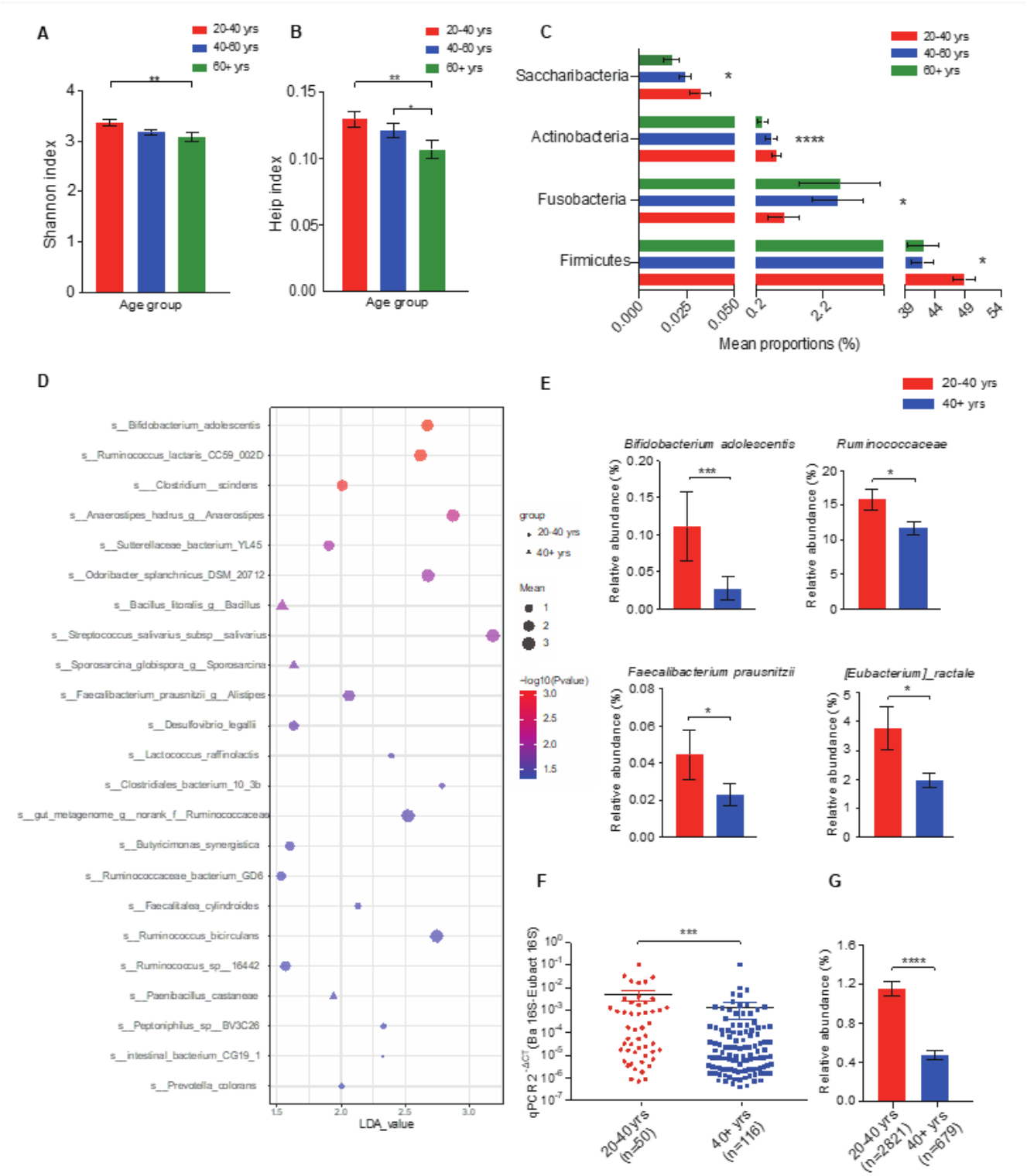

Figure 1

Alteration of gut microbiota diversity and B. adolescentis abundance with aging. (A and B) Alpha-diversity estimators shannon index (A) and heip index (B) of human fecal samples in three age groups of 20-40, 40-60 and >60 years old, respectively . (C) Relative abundance of bacterial taxa in different age groups at

phylum level. (D) Linear discriminant analysis (LDA) coupled with effect size measurements of differentially enriched bacterial taxa at species level. The horizontal coordinate axis represents the LDA value, and the longitudinal coordinate axis represents -log10 (P-value). Larger sizes and darker colors represent higher mean abundance and more significant abundance difference, respectively. (E) Comparison of relative abundance of bacterial taxa associated with short chain fatty acids production. (F and G) Comparison of B. adolescentis abundance by quantitative real-time PCR (F) or 16S rRNA sequencing data shared at GMrepo database (G). Data were shown as mean ±SEM. Wilcoxon rank sum test was performed between two groups and Kruskal-Wallis test was performed among three groups. *p<0.05; **p<0.01; ***p<0.001; ****p<0.0001.

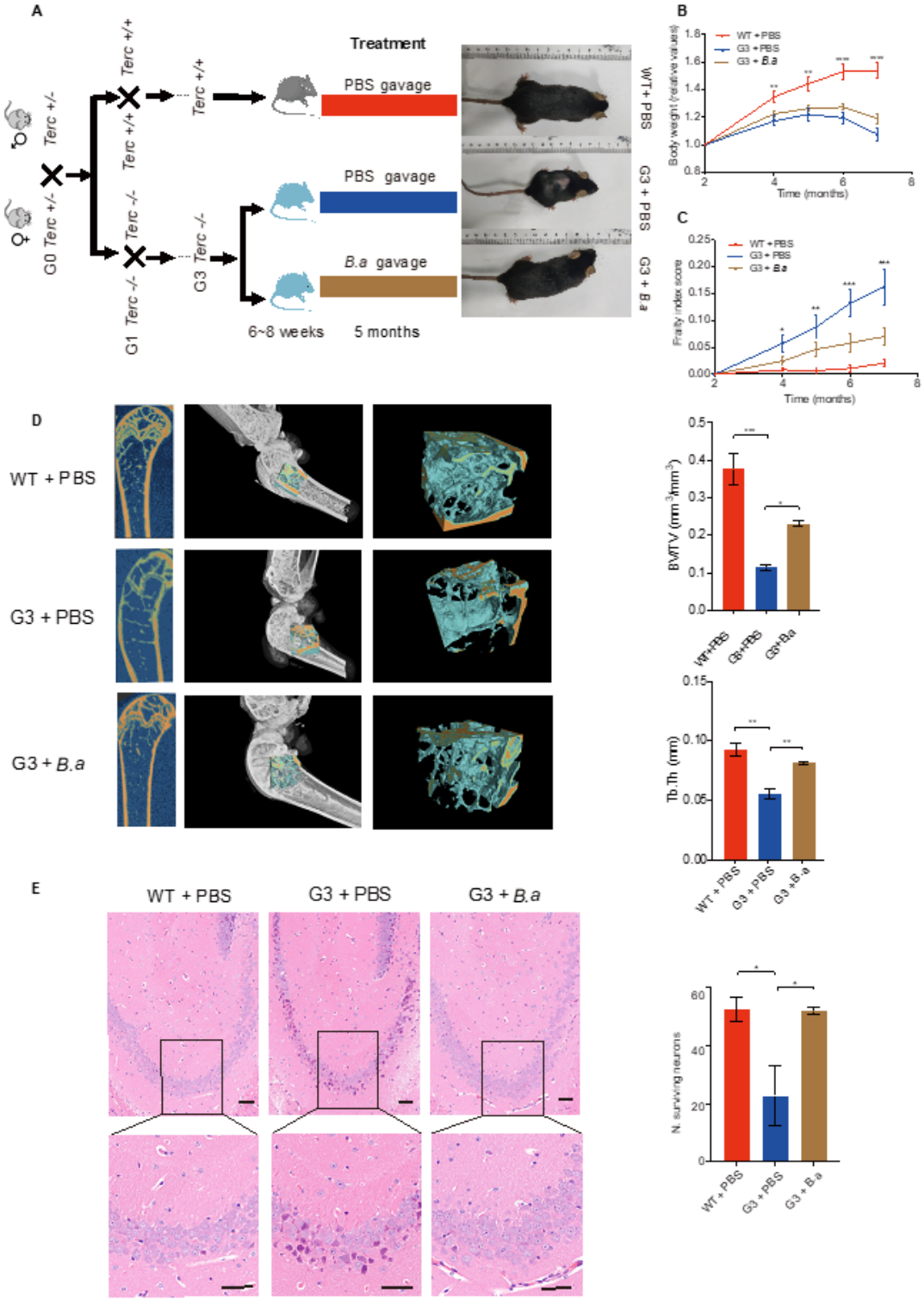

Figure 2

B. adolescentis alleviated the aged related osteoporosis and neurodegeneration in Terc-/- mice. (A) Terc+/- G0 mice (C57BL/6) were intercrossed to generate Terc+/+ (wild-type C57BL/6) and Terc-/- G1 mice. The obtained Terc-/- G1 mice were then intercrossed to generate Terc-/- G3 mice and divided into three groups for further studies. 6 to 8-week-old wild-type C57BL/6 littermates were gavaged with PBS (WT+PBS, n=11), Terc-/- G3 littermates were randomly assigned to PBS gavage group (G3+PBS, n=9) and

B. adolescentis gavage group (G3+B.a, n=12). Mice were gavaged every other day until natural death or sacrifice at 7 months old. (B and C) Curves of relative values of body weight (B) and frailty index score (C). (D) Bone masses were tested by micro-computed tomography (micro-CT) and three-dimensional images were reconstructed. The “interesting zone” was magnified. Bone volume/total volume (BV/TV) and trabecular thickness (Tb.Th) were analyzed with the VGSTUDIO MAX software. n=3 each group. (E) Representative images of hematoxylin and eosin staining of the hippocampal CA3 region. Scale bar, 100μm. The black boxes indicate the area magnified in the bottom. Scale bar, 50μm. The number of surviving neurons in the hippocampal CA3 region were compared as well. Data were shown as mean±SEM and one-way ANOVA was performed. *p<0.05; **p<0.01; ***p<0.001; ****p<0.0001; n.s., not significant.

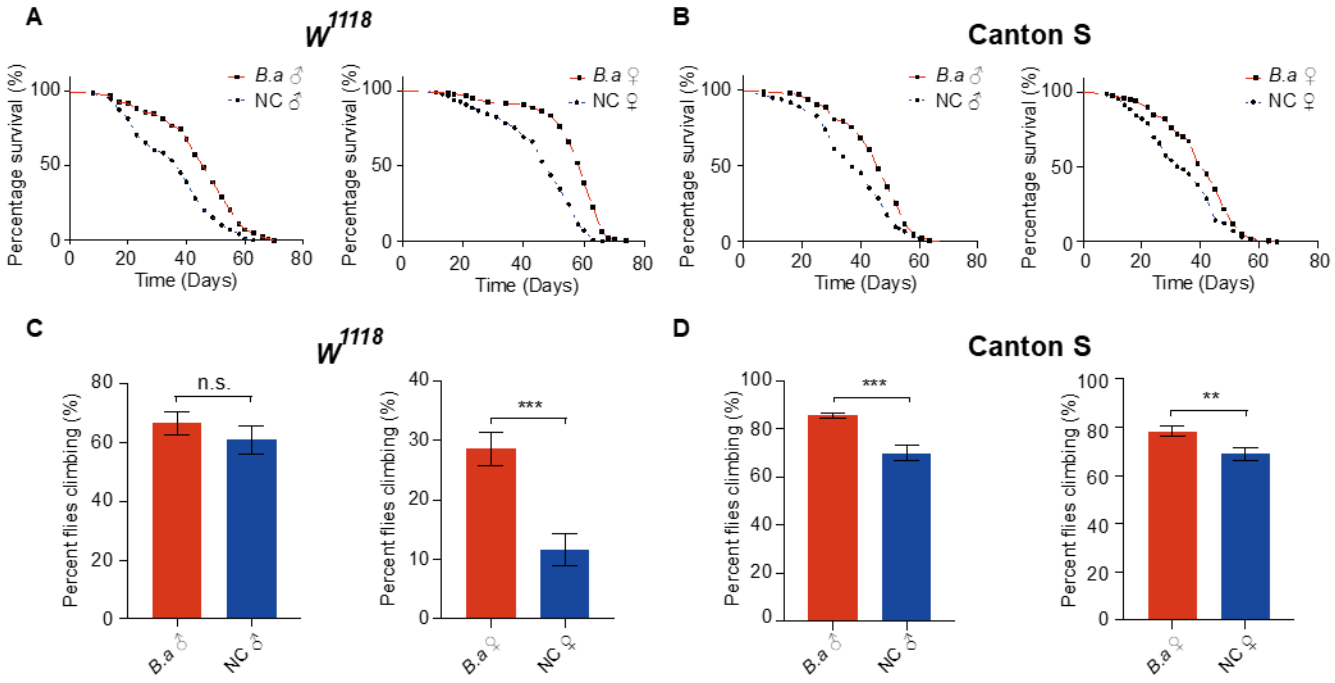

Figure 3

B. adolescentis supplement promoted longevity in Drosophila melanogaster. (A and B) Survival curves of wild-type Drosophila strains w1118 (A) and strain Canton-S (B) supplemented with B. adolescentis (B.a) or 2.5% sucrose solution (NC). n=100 flies each group. (C and D) Comparison of climbing ability of wild-type Drosophila strains w1118 (C) and strain Canton-S (D) supplemented with B. adolescentis (B.a) or 2.5% sucrose solution (NC) at day 30. n=100 flies each gender. Data were shown as mean±SEM and Student’s t-test was performed. **p<0.01; *** p<0.001; ****p<0.0001; n.s., not significant.

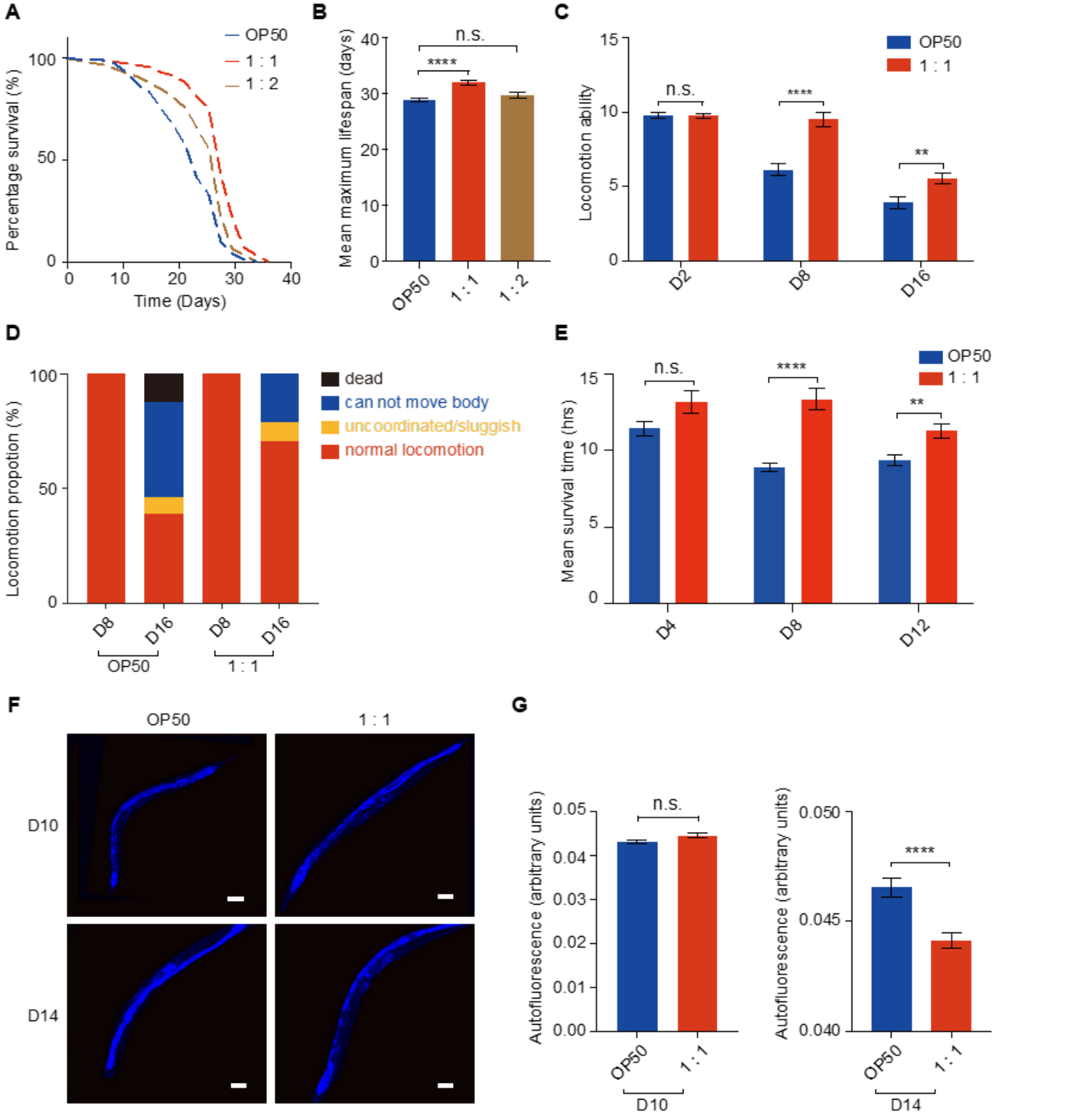

Figure 4

B. adolescentis induced lifespan extension and healthspan improvement in C. elegans. (A and B) Survival curves (A) and mean maximum lifespan (B) of wild-type C. elegans strain N2 fed on E. coli OP50, 1:1 or 1:2 mixture of E. coli OP50 and B. adolescentis, respectively. n=150 worms each group. (C) Locomotion ability quantification of N2 fed on E. coli OP50 or 1:1 mixture of E. coli OP50 and B. adolescentis on day 2, day 8 and day16, respectively. n=50 each group. (D) Locomotion ability classification of N2 fed on E.

coli OP50 or 1:1 mixture of E. coli OP50 and B. adolescentis on day 8 and day 16. class “A”: represents for spontaneous movement or vigorous locomotion in response to stimuli; class “B”: not move unless touched or appeared to have uncoordinated movement; class “C”: moved only head and/or tail in response to stimuli; class “D”: dead. n=50 each group. (E) Mean survival time of N2 fed on E. coli OP50 or 1:1 mixture of E. coli OP50 and B. adolescentis under heat stress on day 4, day 8 and day 12. n=30 each group. (F and G) Representative images of autofluorescence (F) and quantitative comparison (G) of lipofuscin accumulation. n≥20 each group; scale bar, 100μm. Data were shown as mean±SEM and Student’s t-test was performed. **p<0.01; ****p<0.0001; n.s., not significant.

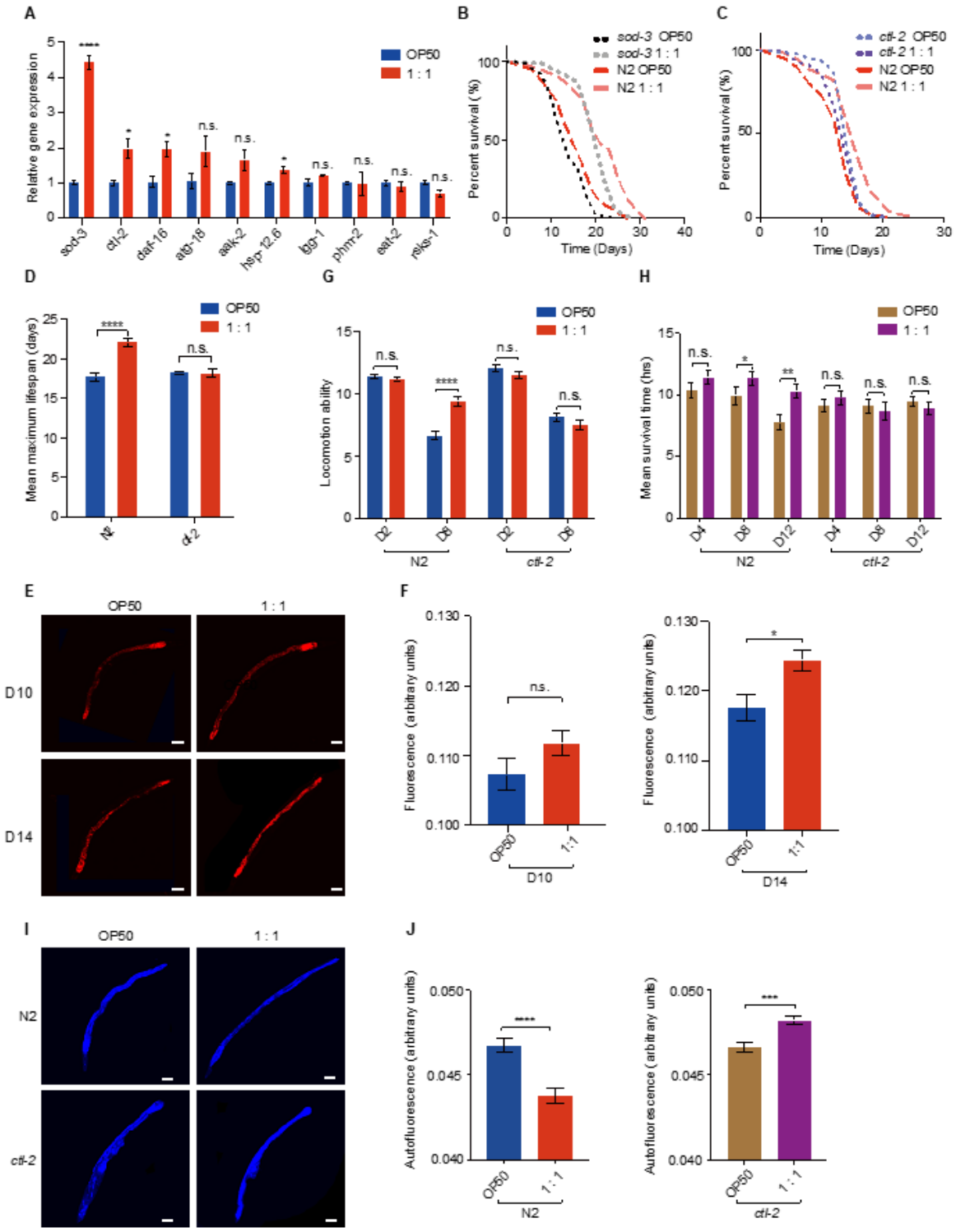

Figure 5

ctl-2 is essential for lifespan and healthspan by B. adolescentis in C. elegans. (A) Relative mRNA expression of aging-associated genes in C. elegans strain fed on E. coli OP50 or 1:1 mixture of E. coli OP50 and B. adolescentis. (B and C) Survival curves of C. elegans mutants sod-3 (B) and ctl-2 (C) compared to wild-type strain N2. n=150 worms each group. (D) Mean maximum lifespan of N2 and ctl-2 mutant. (E and F) Representative images of mCherry fluorescence of ctl-2 expression (E) and quantitative

comparison (F) in N2 on day 10 and day 14. n≥20 each group, scale bar, 100μm. (G) Locomotion ability quantification of N2 and ctl-2 mutant on day 2 and day 8. n=50 each group. (H) Mean survival time of N2 and ctl-2 mutant under heat stress on day 4, day 8 and day 12, respectively. n=30 each group. (I and J) Representative images of autofluorescence (I) and quantitative comparison (J) of lipofuscin accumulation on day 14. n≥20 each group, scale bar, 100μm. Data were shown as mean±SEM and Student's t-test was performed. *p<0.05; **p<0.01; ***p<0.001; ****p<0.0001; n.s., not significant.

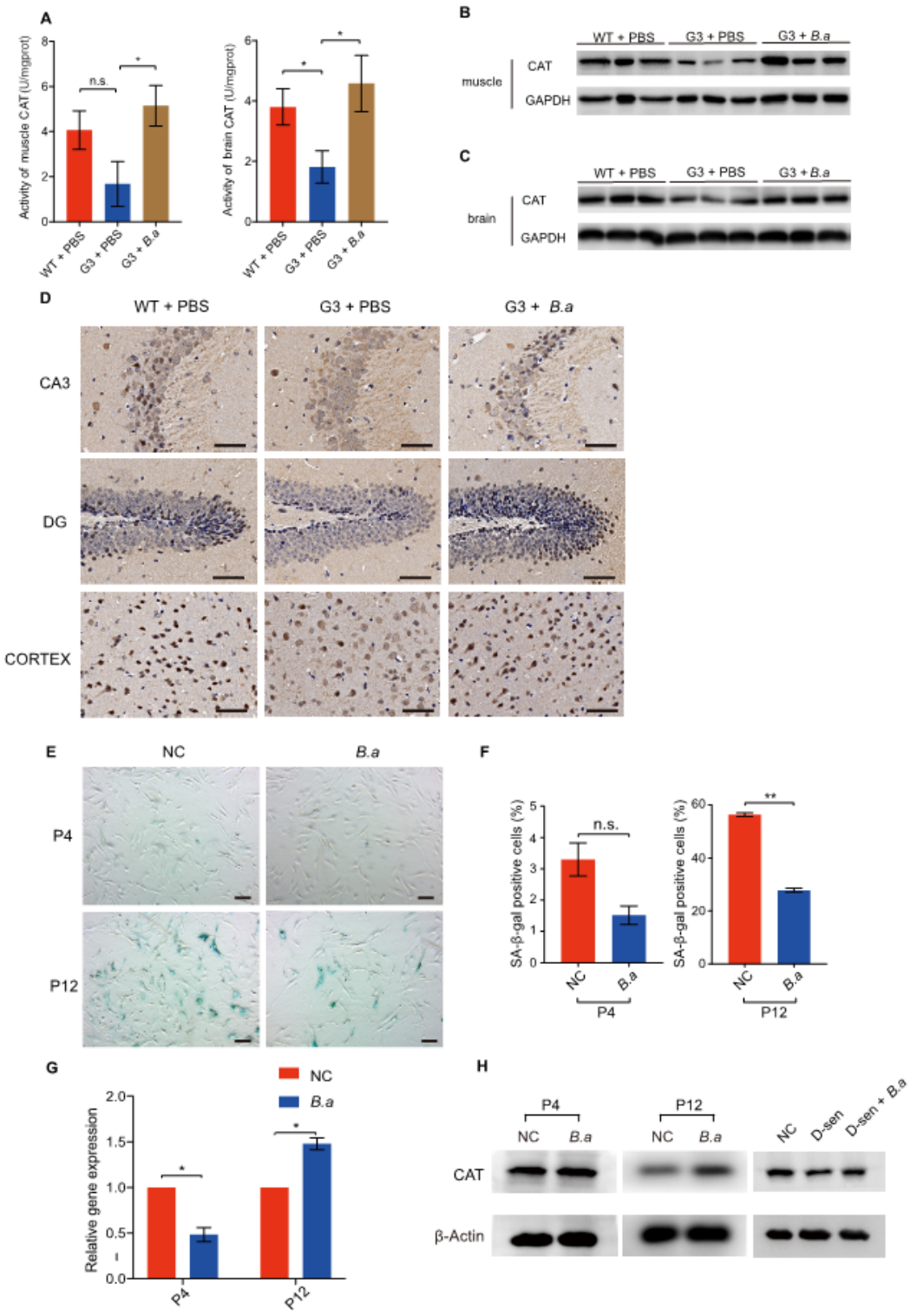

Figure 6

B. adolescentis supplement improved healthspan of Terc-/- mice and suppressed MEFs cellular senescence by regulating the activity of CAT. (A) CAT activity in muscle and brain homogenate of 7-month-old mice was measured and compared among wild-type mice gavage with PBS (WT+PBS, n=10), Terc-/- G3 mice gavaged with PBS (G3+PBS, n=6) and Terc-/- G3 mice gavaged with B. adolescentis (G3+B.a, n=9). (B and C) Immuno-staining of CAT in muscle (B) and brain tissues (C) in mice. (D) Representative images of immunohistochemistry staining of CAT in brain region including hippocampal CA3, DG region and cortex. Scale bar, 50μm. (E and F) Representative images of senescence-associated β-galactosidase (SA-β-gal) staining of replicative senescent MEFs supplemented with PBS (NC) or B. adolescentis (B.a) at passage 4 (P4) and passage 12 (P12) (E) and corresponding percentage evaluation of SA-β-gal-positive cells (F). Scale bar, 100μm. (G) Quantitative real-time PCR of CAT expression in replicative senescent MEFs at P4 and P12. (H) Expression of CAT in replicative and DOX-induced senescent MEFs supplemented with PBS (D-sen) or B. adolescentis (D-sen+B.a). Data were shown as mean±SEM and Student’s t-test was performed. *p<0.05; **p<0.01; n.s., not significant. DOX, doxorubicin.

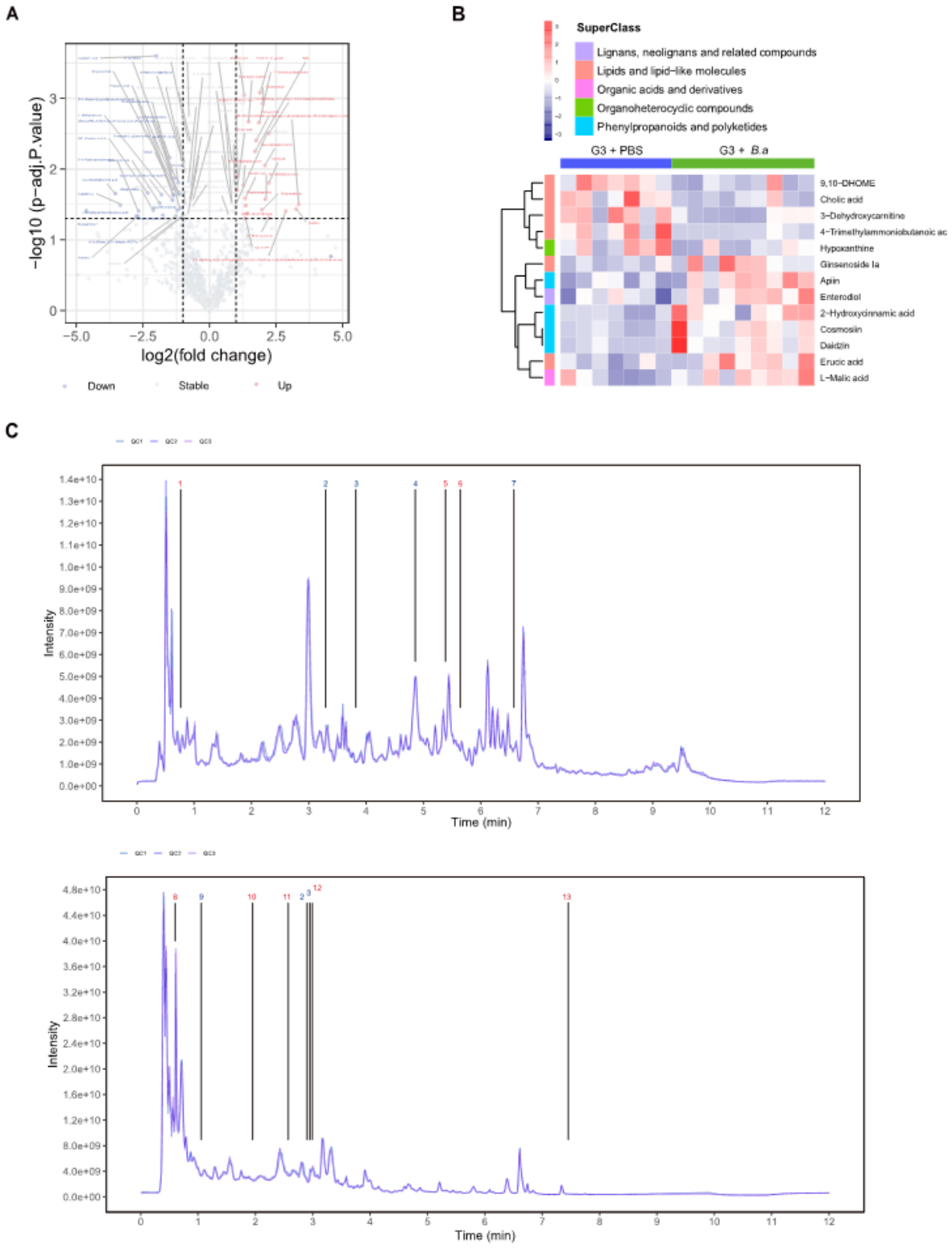

Figure 7

B. adolescentis regulated oxidative stress-associated metabolites in Terc-/- mice. (A) The volcano plot of the gut metabolites analysis of Terc-/- G3 mice gavage with PBS (n=7) or B. adolescentis (n=9). The labeled data points show the abundance of metabolites with two fold or more difference. Red boxes represent enrichment of metabolites in the feces of mice gavage with B. adolescentis, blue box represents enrichment of metabolites in the feces of mice gavage with PBS. (B) Heatmap of hierarchical clustering

analysis. The blue or red boxes indicate the fold change of metabolites abundance less or more than the mean. G3+PBS, Terc-/- G3 mice gavage with PBS, n=7; G3+B.a, Terc-/- G3 mice gavage with B. adolescentis, n=9. (C) Total ion chromatography (TIC) diagrams in positive and negative ion mode of quality control (QC) sample. 1, Ginsenoside Ia; 2, Cholic acid; 3, Hypoxanthine; 4, 4-Trimethylammoniobutanoic acid; 5, Enterodiol; 6, Apiin; 7, 3-Dehydroxycarnitine; 8, Erucic acid; 9, 9,10-DHOME; 10, Cosmosiin; 11, Daidzin; 12, 2-Hydroxycinnamic acid; 13, L-Malic acid. Metabolites in red were found in higher concentrations in Terc-/- G3 mice gavage with B. adolescentis; metabolites in blue were found in higher concentrations in Terc-/- G3 mice gavage with PBS.

Supplementary Files

This is a list of supplementary files associated with this preprint. Click to download.

- Supplementayfiles.pdf
- SupplementaryFigures.docx